Intermetallics 97 (2018) 77–84

Contents lists available at ScienceDirect

Intermetallics

journal homepage: www.elsevier.com/locate/intermet

Liquid phase separation phenomena in $Al_{2.2}CrCuFeNi_2$ HEA

A. Munitz[a,*], S. Samuha[a], E. Brosh[a], S. Salhov[a], N. Derimow[b], R. Abbaschian[b]

[a] Nuclear Research Center-Negev, P.O. Box 9001, Beer-Sheva 841900, Israel
[b] College of Engineering, University of California, Riverside, CA 92521, USA

ARTICLE INFO

Keywords:
Stable miscibility gap
Constitutional liquid phase separation
Two liquids
Rosette structure
Sigma phase
Spinodal decomposition

ABSTRACT

Vacuum arc melting was used to produce buttons of $Al_{2.2}CrCuFeNi_2$ HEA. High resolution scanning electron microscopy (SEM) with energy dispersive X-ray spectroscopy (EDS) capabilities as well as X-ray diffraction (XRD) were used for microstructural characterization. The alloy solidified dendritically with rosette structure of dendritic core (DC) regions composed of at least 3 concentric circles or semicircles with different phases and morphology. First to solidify was found to be a supersaturated solid solution with matrix B2 structure that underwent spinodal decomposition as the alloy cooled during solidification. The B2, matrix which initially contained nanosize cubical disordered BCC precipitates, later changed to nanosize rectangles (2nd circle), and eventually to micron-size elongated non-faceted precipitates. This was followed by the solidification of the residual Cu-rich liquid in the interdendritic (ID) regions, which separated into two liquids (LPS) upon rejection of more solute into the liquid. We term this liquid phase separation as "constitutional LPS" in contrast with thermal LPS that takes place during cooling of stable or metastable monotectic alloys. Nevertheless, the constitutional LPS was not predicted using the existing thermodynamic databases.

1. Introduction

Recently, Guo et al. [1] synthesized a Co-free $Al_xCrCuFeNi_2$ (x ranging between 0.2 and 2.5) in which the hardness increased with increasing Al concentration [1]. They reported on an anomalous solidification microstructure of sunflower-like structures observed in $Al_{2.2}CrCuFeNi_2$. However, the article did not provide a reasonable explanation to the unique microstructure. Since liquid phase separation (LPS) has been observed in several high-entropy alloys (HEA) [2,3], we would like to investigate if the $Al_{2.2}CrCuFeNi_2$ alloy undergoes a similar liquid phase separation.

Since the pioneering work of Nakagawa on liquid phase separation in Cu-Fe and Cu-Co alloys [4] much research has been conducted to investigate LPS in binary alloys such as Cu-Fe [5,6], Cu-Co [7–10], Cu-Cr [11], Cu-Nb [12] and ternary alloys Cu-Co-Fe [13–16], Cu-Fe-Si [17] and Ag-Ni-Nb [18]. More recent liquid phase separation has also been observed in HEAs such as in AlAgCoCrCuNi and AlAgCoCrCuFeNi alloys [19] and later confirmed by Munitz et al. [3]. Stable LPS was also found in $CoCrCu_xFeMoNi$ when $x \geq 0.5$ [20] and in $CoCrCuFe_{0.5}Ni$ and $CoCrCuFeNi_{0.5}$ alloys [21]. On the other hand, Liu et al. [22] reported metastable LPS in $CoCrCuFe_xNi$ (x between 1 and 2) alloys when a critical supercooling of 160, 190, and 293 K was reached for alloys with x equal 1, 1.5 and 2, respectively. Wang et al. [23] reported metastable LPS in a CoCrCuFeNi HEA when supercooled beyond 223 K. Recently it was reported that quenching $La_{27.5}Zr_{27.5}Al_{25}Cu_{10}Ni_{10}$ caused LPS into amorphous Zr-Ni-Al and La-Cu-Al metallic glasses [24]. He et al. [25] used the Zr–Ce–La system which has a miscibility gap to synthesize a new Zr–Ce–La–Al–Co monotectic system which underwent LPS into two bulk metallic glasses (LPS-BMGs) during cooling in copper mold through the gap. In addition, Concustell et al. [26] reported that amorphous Ni-Nb-Y system underwent LPS into Ni-Y and Ni-Nb melts. Also, Munitz et al. [2] reported on several HEAs that underwent stable LPS, sometimes with secondary LPS in one or both liquids. Additions of Co, Al, Ti, and Ni to CoCrCuFe alloy, which exhibit metastable LPS, were found to lower the miscibility gap temperature (T_{MG}), while additions of Cr, V, and Nb were observed to raise T_{MG} and enhance the formation of stable LPS (i.e. essentially creating monotectic phase diagram). The influence of the different elements on the miscibility gap temperature in the HEAs investigated was found to be similar to that reported by Wang et al. [27]. The common characteristic microstructures of alloys that exhibit LPS are spheres of the minority liquid embedded in the matrix of other liquid [3,14,28].

The purpose of this work is to achieve a better understanding of the microstructure of arc-cast $Al_{2.2}CrCuFeNi_2$ HEA and investigate if the Rosette (sunflower-like) microstructure originated from LPS and compare the experimental results with thermodynamic simulations of a stable solidification mode.

* Corresponding author.
E-mail address: munitzabr@gmail.com (A. Munitz).

https://doi.org/10.1016/j.intermet.2018.04.004
Received 27 October 2017; Received in revised form 1 April 2018; Accepted 3 April 2018
Available online 07 April 2018
0966-9795/

Table 1
Nominal and measured compositions (in at. %.) of the HEA used in this investigation (EDS analysis).

Element	Average composition	
	Nominal	Measured
Al	30.6	30.7
Cr	13.9	13.9
Fe	13.9	13.9
Ni	27.7	26.2
Cu	13.9	15.3

1.1. Experimental procedure

An $Al_{2.2}CrCuFeNi_2$ HEA was prepared via non-consumable electrode arc melting in a Ti-gettered argon atmosphere. Elemental metal pieces (purity > 99.5%) were inserted into a Cu hearth with Cr or Cr + Fe placed on top of the pile of the other elemental pieces. The chamber was evacuated with a rotary pump to about 4–6 Pa at which point commercial high purity argon gas was introduced into the chamber up to a pressure of 2 KPa and then purged back to a vacuum. This process was repeated to achieve a more inert atmosphere for the process. After arc ignition, the Ti getter was melted first, followed by melting of the alloying elements for about 30 s. The buttons were flipped over and the melting process was repeated 5 times to improve the chemical homogeneity. The dimensions of the buttons after melting were about 20 mm in diameter and a maximum height of about 10 mm. The buttons were cross-sectioned into 4 mm-wide strips for microstructure examination. The nominal and measured compositions are shown in Table 1.

The metallographic specimens were mounted in phenolic, abraded on SiC papers up to 4000 grit and then polished with the final polish on a Buehler Vibromet using 0.05 μm colloidal silica for 16–20 h. The colloidal silica, being a slightly alkaline solution, has been found to preferentially etch the Cu-rich phases in these HEAs. Therefore, no additional etchant was applied prior to examination using a Field-Emission Scanning Electron Microscope (FESEM) equipped with Energy Dispersive Spectroscopy (EDS) capabilities. For the EDS measurements, the raw intensity data were ZAF corrected an accuracy of ± 0.4 at% for the elements studied [29].

XRD patterns of polished and un-etched samples were recorded on Rigaku RINT 2100 diffractometer with Cu Kα radiation (λ = 0.15406 nm). Data were acquired from 20 to 100° 2θ with a step size of 0.02° and step time of 15 s/step.

1.2. Thermodynamic calculations

A dedicated thermodynamic database was constructed for analyzing the solidification sequence in $Al_{2.2}CrCuFeNi_2$ HEA. The construction of the Al-Cr-Cu-Fe-Ni data was based on thermodynamic published models including the following ternary systems: Al-Cr-Fe [30], Al-Cr-Ni [31], Al-Cu-Fe [32], Al-Cu-Ni [33], Al-Fe-Ni [34], Cr-Cu-Fe [35], Cr-Cu-Ni [36], Cr-Fe-Ni, Cu-Fe-Ni [37] [38]. Only the liquid, FCC-A1, BCC-A2, and B2 phases were modeled since these phases appear during solidification. The database was validated by calculating and relating the binary and ternary phase diagrams, and comparing them to the original assessments [30–32,34–39]. In addition, multicomponent calculations were performed for $Al_xCrCuFeNi_2$ (were x ranges between 0 and 3) and were compared to the results of Liu et al. [40] who used Pandat software, and Andersson et al. [41] and Choudhuri et al. [42] which used Thermo-Calc TCHEA1 database. We have found that our calculations agreed with those made with these commercial databases therefore, our calculations were validated.

After validating the database, we performed calculations using Thermo-Calc software [41] based on Scheil solidification assumptions of fast diffusion in the liquid and negligible diffusion in the solid [43] as well as equilibrium conditions at the interface. We used the database to calculate the different phases that can exist over a temperature range in two ways: solidification under equilibrium conditions, and solidification according to Scheil approach.

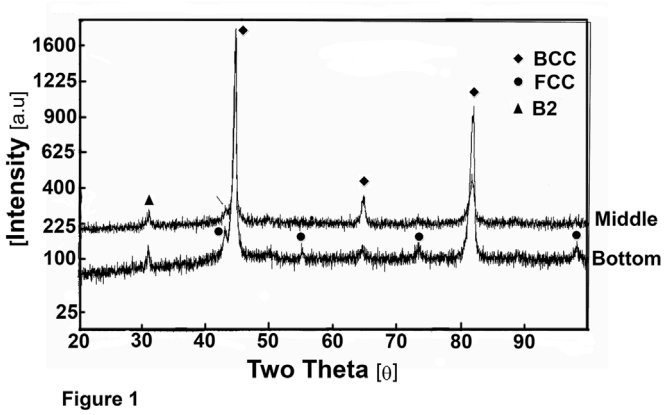

Fig. 1. XRD patterns from the $Al_{2.2}CrCuFeNi_2$ alloy in the as-cast condition in two locations: 1 mm and 6 mm from the bottom.

2. Results

2.1. X-ray diffraction (XRD) results

XRD diffractograms from two locations parallel to the bottom of the cast button in the as cast condition is shown in Fig. 1: One scan was done about 1 mm from the bottom and the other in the middle of the cast (around 6 mm from the bottom). As indicated the structure of the middle of the as-cast alloy composed of a BCC structure with a small extra peak near 31° corresponding to the (001) reflection of the ordered BCC (i.e. B2) phase as well as indication of small FCC phase near 45° (indicated by an arrow). In contrast, the bottom of the cast displayed an FCC phase in addition to the BCC and B2 phases.

2.2. Microstructural characterization

Backscattered electron images (BSI) illustrating the microstructure of a cross section parallel to the cast bottom at 1 mm from the copper chill are shown in Fig. 2. Two different regions can be observed in the figure: the brighter region marked as P-L2, located near the edge indicating higher atomic average, and the other darker region, marked with P-L1, with lower atomic average. The P-L1 region contained the Rosette (sunflower-like microstructure) similar to that reported by Guo et al. [1] shown in Fig. 2c.

Detailed analysis indicates that the microstructure of L2 consisted of grains with Cu rich regions decorating the grain boundaries while darker spheres are embedded in the grains and grain boundaries. The average compositions of the P-L2 region, i.e., the bright matrix, and the dark spheres, are summarized in Table 2. The microstructure of regions marked P-L1 have the morphology of the sunflowers reported by Guo et al. [1]. The appearance of spheres of one composition completely different from the matrix is indicative of LPS, and will be discussed. The spheres are separated due to further cooling in the P-L2 and termed as secondary LPS-S-L1.

Secondary electron images (SEI) illustrating the microstructure of the dark areas, marked as P-L1 in Fig. 2a, at a higher resolution are seen in Fig. 3. The microstructure consisted of cells composed of 3 concentric circles (Fig. 3a) or semi-circles marked 1, 2, and 3 in Fig. 3b. In between those cells are areas with different microstructure marked as 4 in Fig. 3b and in higher magnification in top right of Fig. 3d and e. The microstructure of the first circle (1 in Fig. 3b) usually is smooth (Fig. 3c), however nanosize cubical precipitates are sometimes found